

# Edge-Functionalization of Pyrene as a Miniature Graphene via Friedel–Crafts Acylation Reaction in Poly(Phosphoric Acid)

In-Yup Jeon · Eun-Kyoung Choi · Seo-Yoon Bae ·  
Jong-Beom Baek

Received: 4 June 2010 / Accepted: 1 July 2010 / Published online: 15 July 2010  
© The Author(s) 2010. This article is published with open access at Springerlink.com

**Abstract** The feasibility of edge-functionalization of graphite was tested via the model reaction between pyrene and 4-(2,4,6-trimethylphenoxy)benzamide (TMPBA) in poly(phosphoric acid) (PPA)/phosphorous pentoxide ( $P_2O_5$ ) medium. The functionalization was confirmed by various characterization techniques. On the basis of the model study, the reaction condition could be extended to the edge-functionalization of graphite with TMPBA. Preliminary results showed that the resultant TMPBA-grafted graphite (graphite-g-TMPBA) was found to be readily dispersible in *N*-methyl-2-pyrrolidone (NMP) and can be used as a precursor for edge-functionalized graphene (EFG).

**Keywords** Pyrene · Graphite · Graphene · Edge-functionalization

## Introduction

Graphene, a single layer of carbon atom bonded together in a hexagonal lattice, has attracted tremendous attention due to its peculiar electronic and physical properties [1–6]. However, there are two issues that have to be resolved first for its use in practice. The one is scalable exfoliation of graphite into graphene and/or graphene-like sheets (less than ten layers) [7]. The other is stabilization of exfoliated graphene suspension in various matrices [8]. Graphite oxide (GO), which is oxidized form of graphite containing oxygenated functional groups on its edge and basal plane,

has been considered the most viable chemical approach for the mass production of graphene [9]. However, GO has inherent problem in reversing to graphene structure, because the reduction conversion from GO into reduced graphene oxide (rGO) is limited to ~70%, implying that rGO still contains ~30% of oxygenated defects [10]. Thus, an important remaining challenge is still the development of new chemical method to produce large quantity and high quality graphene in large quantities. We believe that one promising chemical approach is the edge-functionalized graphite (EFG) via Friedel–Crafts acylation reaction. Unlike GO, the EFG is exclusively functionalized at the edge, where  $sp^2C-H$  is located [11]. As a result, the interior graphene crystalline structure is undamaged and its characteristic properties are preserved. In addition, the EFG is expected to be efficiently dispersed and stabilized in common organic solvents to give graphene-like sheets.

Herein, we would like to report the edge-chemistry of graphene via the model reaction between pyrene as a miniature graphene and 4-(2,4,6-trimethylphenoxy)benzamide (TMPBA) as a molecular wedge. The reaction condition, poly(phosphoric acid) (PPA)/phosphorous pentoxide ( $P_2O_5$ ) medium at 130 °C, was previously optimized for the “direct” functionalization of carbon-based nanomaterials such as carbon nanotubes and carbon nanofibers [12–20]. The result from the model reaction could give an insight for predicting edge-chemistry of graphene.

## Experimental Section

### Materials

All reagents and solvents were purchased from Aldrich Chemical Inc. and used as received, unless otherwise mentioned.

I.-Y. Jeon · E.-K. Choi · S.-Y. Bae · J.-B. Baek (✉)  
Interdisciplinary School of Green Energy, Institute of Advanced  
Materials & Devices, Ulsan National Institute of Science and  
Technology (UNIST), 100, Banyeon, Ulsan 689-798, South  
Korea  
e-mail: jbbaek@unist.ac.kr

4-(2,4,6-Trimethylphenoxy)benzamide (TMPBA) was synthesized by literature procedure [21]. Graphite (Cat#: 496596, type: powder, particle size: <45 µm, purity: 99.99+%) was obtained from Aldrich Chemical Inc. and used as received.

### Instrumentation

Infrared (FT-IR) and FT-Raman spectra were recorded on a Bruker Fourier transform spectrophotometer IFS-66/FRA106S. The field emission scanning electron microscopy (FE-SEM) was performed on FEI NanoSEM 200. Matrix-assisted laser desorption ionization time of flight (MALDI-TOF) from Bruker Ultraflex III was used for mass analysis. <sup>1</sup>H and <sup>13</sup>C NMR were conducted with Varian VNMRs 600. Elemental analysis (EA) was conducted with Thermo Scientific Flash 2000. X-Ray photoelectron spectroscopy (XPS) was performed on Thermo Fisher K-alpha.

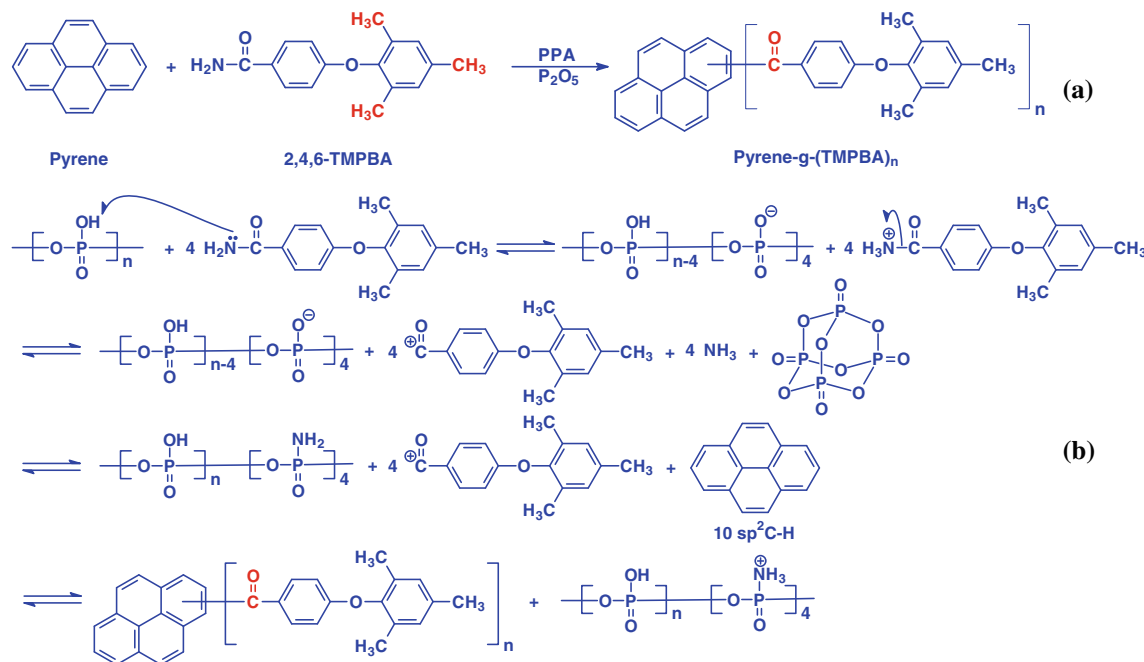
### General Procedure for the Functionalization of Pyrene with 4-(2,4,6-Trimethylphenoxy)Benzamide (TMPBA) in Polyphosphoric Acid (PPA)/Phosphorous Pentoxide ( $P_2O_5$ )

Into a 250-mL resin flask equipped with a high-torque mechanical stirrer, the nitrogen inlet and outlet, pyrene (0.5 g, 2.47 mmol), 4-(2,4,6-trimethylphenoxy)benzamide (0.5 g, 1.96 mmol), PPA (83%  $P_2O_5$  assay: 20.0 g) and

$P_2O_5$  (5.0 g) were placed and stirred under dry nitrogen purge at 130 °C for 72 h. The initial white mixture became pinkish-white as the functionalization reaction progressed. At the end of the reaction, the color of the mixture turned to violet, and the reaction mixture was poured into distilled water. The resultant brown precipitates were collected by suction filtration, Soxhlet-extracted with water for 3 days to completely remove reaction medium and then with methanol for three more days to get rid of unreacted pyrene and TMPBA. Finally, the sample was freeze-dried under reduced pressure (0.5 mmHg) at –120 °C for 72 h to give 0.74 g (79% yield) of greenish-brown powder. Anal. Calcd. for  $C_{48}H_{38}O_2$  (pyrene-g-TMPBA<sub>2</sub>): C, 84.93%; H, 5.64%; O, 9.43%. Found: C, 84.69%; H, 5.25%; O, 7.58%.

### Results and Discussion

As presented in Scheme 1a, pyrene and TMPBA were treated in PPA/ $P_2O_5$  at 130 °C for 48 h. Then, the reaction mixture was poured into distilled water to isolate light greenish-brown powder. The reason for using TMPBA is to prevent self-reaction by blocking 2, 4 and 6 positions to the aromatic ether-activated sites for electrophilic substitution reaction. To avoid unexpected variables, the resultant products were completely worked-up by Soxhlet extraction with water for 3 days to remove reaction medium and with methanol for 3 days to get rid of unreacted TMPBA and low molar mass impurities (see “Experimental Section”).



**Scheme 1** **a** The reaction between pyrene and TMPBA in poly(phosphoric acid)/phosphorous pentoxide at 130 °C; **b** proposed mechanism of a “direct” Friedel–Crafts acylation reaction between acylium ion ( $\text{Ph-C}^+=\text{O}$ ) of TMPBA and  $\text{sp}^2\text{C-H}$  of pyrene

The isolated pyrene-g-(TMPBA)<sub>n</sub> was freeze-dried ( $-120^{\circ}\text{C}$ ) under reduced pressure ( $10^{-2}$  mmHg). The proposed mechanism of the electrophilic substitution reaction is a “direct” Friedel–Crafts acylation reaction between acylium ion ( $\text{Ph}-\text{C}^+=\text{O}$ ) of TMPBA and  $\text{sp}^2\text{C}-\text{H}$  of pyrene to give pyrene-g-(TMPBA)<sub>n</sub> (Scheme 1b).

FT-IR was used as convenient tool to identify chemical bonds in pyrene-g-(TMPBA)<sub>n</sub>. If there are free standing TMPBA and pyrene as residual impurities, there must be trace of carbonyl ( $\text{C}=\text{O}$ ) stretching peak at  $1,642\text{ cm}^{-1}$  and amide peaks at  $3,215$  and  $3,386\text{ cm}^{-1}$  arising from benzamide, and  $\text{sp}^2\text{C}-\text{H}$  peak at  $3,044\text{ cm}^{-1}$  from pyrene (Fig. 1a). However, pyrene-g-(TMPBA)<sub>n</sub> does not show benzamide carbonyl and amine peaks, indicating it does not contain residual impurities, while it does show relatively much weaker  $\text{sp}^2\text{C}-\text{H}$  and new  $\text{sp}^3\text{C}-\text{H}$  peaks around  $2,921\text{ cm}^{-1}$  due mainly to TMPBA and distinct aromatic carbonyl ( $\text{C}=\text{O}$ ) stretching peak at  $1,656\text{ cm}^{-1}$ . Hence, it is evident that most of TMPBA is covalently attached to the edge of pyrene. However, we cannot reliably calculate the graft density of TMPBA onto pyrene edges.

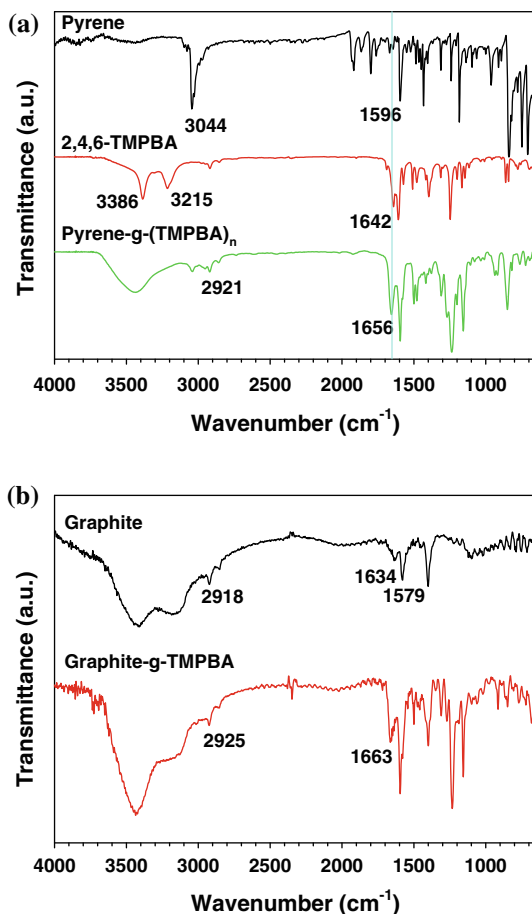


**Fig. 1** FT-IR (KBr pellet) spectra: **a** pyrene, 4-(2,4,6-trimethylphenoxy)benzamide and pyrene-g-(TMPBA)<sub>n</sub>; **b** graphite and graphite-g-TMPBA

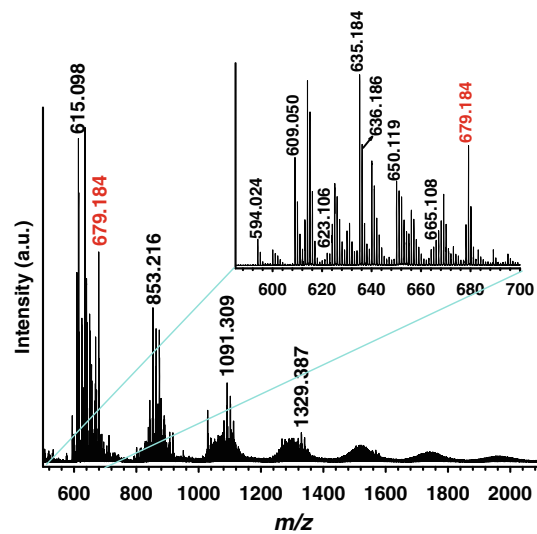


**Fig. 2** MALDI-TOF spectra of pyrene-g-(TMPBA)<sub>n</sub>. Inset is extended from 500 to 700 amu

The covalent attachment of TMPBA onto pyrene could be confirmed by matrix-assisted laser desorption ionization time of flight (MALDI-TOF) analysis (Fig. 2). A series of peak groups appeared, indicating that a mixture of pyrene-g-(TMPBA)<sub>n</sub> ( $n = 2, 3, 4, 5, 6, 7, 8, 9, 10$ ) is present. The peak groups are separated by 238.1 amu, whose value is exact molecular weight of dehydrated [TMPBA]<sup>+</sup> (FW = 238.23 g/mol). The strongest peak group contains 679.2 amu, which is exactly matched to the molecular weight of pyrene-g-(TMPBA)<sub>2</sub>. The highest peak at 615.1 amu corresponds to  $[\text{CH}_3]_4$  losses from pyrene-g-(TMPBA)<sub>2</sub>. Hence, it can be concluded that the highest population in the mixture of pyrene-g-(TMPBA)<sub>n</sub> is pyrene-g-(TMPBA)<sub>2</sub> ( $n = 2$ ).

From elemental analysis, experimental CHO contents are 84.69, 5.25 and 7.58% for pyrene-g-(TMPBA)<sub>n</sub> (Table 1). The values are closest to theoretical CHO values with empirical formula weight of  $\text{C}_{48}\text{H}_{38}\text{O}_4$ , which agreed well with those of pyrene-g-(TMPBA)<sub>2</sub> ( $n = 2$ ). Hence, the bisubstitution of TMPBA onto pyrene could be most likely occurred to pyrene via “direct” Friedel–Crafts acylation reaction.

Although the mixture of pyrene-g-(TMPBA)<sub>n</sub> contains pyrene-g-(TMPBA)<sub>2</sub> as major component, it is still a mixture as referenced by MALDI-TOF analysis. The full assignment of all NMR peaks is technically impossible. Nevertheless, the carbonyl bond ( $\text{C}=\text{O}$ ) between pyrene and TMPBA could be clearly assignable from both <sup>1</sup>H (Fig. 3a) and <sup>13</sup>C-NMR spectra (Fig. 3b). The results further assure the feasibility of the reaction between pyrene and TMPBA.

On the basis of results from model reaction, the covalent attachment of TMPBA on the edge of graphite can be

**Table 1** Empirical formula (EF), formula weight (FW), calculated and experimental elemental analysis of samples

Sample	EF	FW	Elemental analysis		
			C (%)	H (%)	O (%)
Pyrene	C <sub>16</sub> H <sub>10</sub>	202.25	95.02	4.98	0.00
Pyrene-g-(TMPBA) <sub>1</sub>	C <sub>32</sub> H <sub>24</sub> O <sub>2</sub>	440.54	87.25	5.49	7.26
Pyrene-g-(TMPBA) <sub>2</sub>	C <sub>48</sub> H <sub>38</sub> O <sub>4</sub>	678.82	84.93	5.64	9.43
Pyrene-g-(TMPBA) <sub>3</sub>	C <sub>64</sub> H <sub>52</sub> O <sub>6</sub>	917.11	83.82	5.71	10.47
Pyrene-g-(TMPBA) <sub>4</sub>	C <sub>80</sub> H <sub>66</sub> O <sub>8</sub>	1155.39	83.16	5.76	11.08
Pyrene-g-(TMPBA) <sub>5</sub>	C <sub>96</sub> H <sub>80</sub> O <sub>10</sub>	1393.68	82.73	5.79	11.48
Pyrene-g-(TMPBA) <sub>6</sub>	C <sub>112</sub> H <sub>94</sub> O <sub>12</sub>	1631.97	82.43	5.81	11.76
Pyrene-g-(TMPBA) <sub>7</sub>	C <sub>128</sub> H <sub>108</sub> O <sub>14</sub>	1870.25	82.20	5.82	11.98
Pyrene-g-(TMPBA) <sub>8</sub>	C <sub>144</sub> H <sub>122</sub> O <sub>16</sub>	2108.54	82.03	5.83	12.04
Pyrene-g-(TMPBA) <sub>9</sub>	C <sub>160</sub> H <sub>136</sub> O <sub>18</sub>	2346.82	81.89	5.84	12.27
Pyrene-g-(TMPBA) <sub>10</sub>	C <sub>176</sub> H <sub>150</sub> O <sub>20</sub>	2585.11	81.77	5.85	12.38
Pyrene-g-(TMPBA) <sub>n</sub>	C <sub>x</sub> H <sub>y</sub> O <sub>z</sub>	Found	84.69	5.25	7.58

anticipated. Hence, graphite was also treated with TMPBA in the same reaction and work-up conditions. For the purpose of having a basic understanding of the starting material, pristine graphite was characterized by elemental analysis (Table 2). When theoretical C H N O contents were calculated, the negligible amount of edge sp<sup>2</sup>C–H contribution was ignored and C content for pristine graphite was assumed to be 100%. However, the elemental analysis of pristine graphite shows C H N O contents of 98.81, 0.13, 0.00 and 0.00%, respectively. The result allowed us to estimate the amount of available sp<sup>2</sup>C–H for the Friedel–Crafts acylation reaction. The H content, which is most likely from sp<sup>2</sup>C–H at the edges, of graphite, seems minor. However, when it is converted into molar ratio, the C/H ratio becomes 63.8. Thus, the theoretical C H N O values of resultant graphite-g-TMPBA are calculated based on final yield. For example, assuming the amount of graphite before and after reaction remains constant, the amount of TMPBA grafted onto the edge of graphite can be simply estimated by subtracting the feed amount of

**Table 2** Elemental analysis of graphite and graphite-g-TMPBA

Sample		Elemental analysis			
		C (%)	H (%)	N (%)	O (%)
As-received graphite	Calcd.	100.00	0.00	0.00	0.00
	Found	98.81	0.13	BDL*	BDL*
Graphite-g-TMPBA	Calcd.	92.03	2.56	0.00	5.41
	Found	90.41	2.50	BDL*	5.71

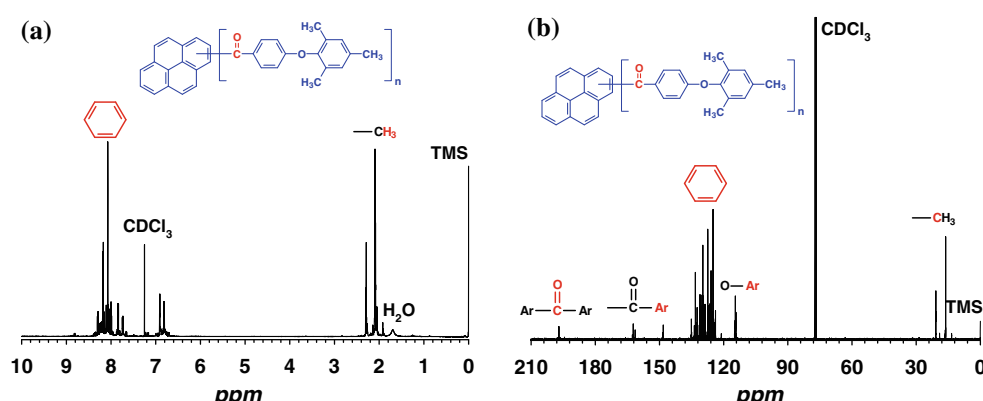
\* BDL below detection limit

graphite. Considering a low experimental C content of as-received graphite (1.19%), a low experimental C content of graphite-g-TMPBA (1.62%) is expected. As a result, it is fair to say that overall experimental CHNO values obtained from graphite-g-TMPBA are agreed well with theoretically calculated values. In addition, the resultant graphite-g-TMPBA does show aromatic carbonyl (C = O) peak at 1,663 cm<sup>-1</sup>, indicating covalent linkage between graphite and TMPBA (Fig. 1b).

The scanning electron microscope (SEM) images of graphite-g-TMPBA and pristine graphite display distinct surface morphology. Pristine graphite shows very smooth surface (Fig. 4a), whereas the surface of graphite-g-TMPBA is relatively rough due to the attachment of TMPBA (Fig. 4b).

Both pristine graphite and graphite-g-TMPBA displayed almost identical the XPS peaks with different intensities (Fig. 5a). Pristine graphite showed a predominant C 1-s peak at 285 eV and much weaker O 1-s peak at 530 eV, presumably arising from physically adsorbed oxygen-containing species in pristine graphite [22], whereas graphite-g-TMPBA showed relatively weaker C 1-s peak and stronger O 1-s peak due to oxygen in carbonyl groups (C = O) together with physically adsorbed one.

As expected, the dispersibility of graphite-g-TMPBA was significantly improved. A red beam from a laser pointer was shined through the graphite-g-TMPBA solution in NMP (0.2 mg/mL) and was able to pass through the dispersed solution, showing Tyndall scattering (Fig. 5b).

**Fig. 3** **a** <sup>1</sup>H NMR (CDCl<sub>3</sub>) spectrum of pyrene-g-(TMPBA)<sub>n</sub>; **b** <sup>13</sup>C NMR (CDCl<sub>3</sub>) spectrum of pyrene-g-(TMPBA)<sub>n</sub>

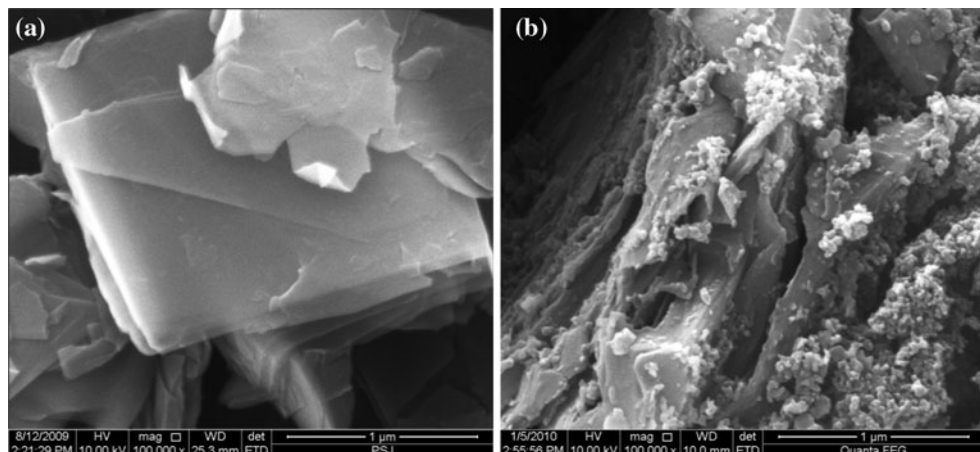
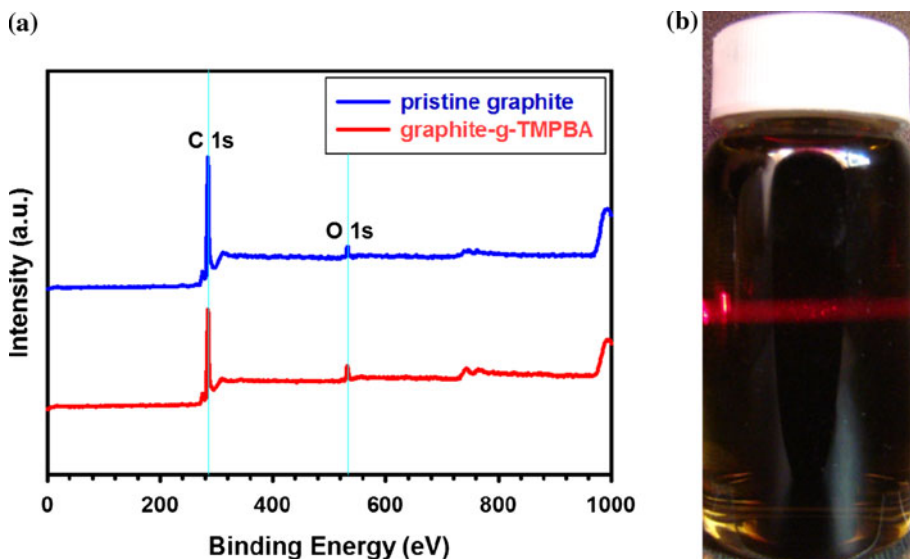


**Fig. 4** **a** SEM image of pristine graphite; **b** SEM image of graphite-g-TMPBA

**Fig. 5** **a** XPS surveys of pristine graphite and graphite-g-TMPBA; **b** photograph of graphite-g-TMPBA dispersed in NMP



The resulting solution remained visually unchanged even after months of standing under ambient condition.

## Conclusions

The model reaction between pyrene as a miniature graphene and 4-(2,4,6-trimethylphenoxy)benzamide (TMPBA) in polyphosphoric acid (PPA)/phosphorous pentoxide ( $P_2O_5$ ) medium was successful for anticipating the edge-chemistry of graphite. The reaction condition was applied for the edge-functionalization of graphite. The resultant graphite-g-TMPBA as an edge-functionalized graphite (EFG) was readily dispersible in *N*-methyl-2-pyrrolidinone (NMP). The result envisions that high quality graphene-like sheets can be synthesized as an alternative approach to problematic graphite oxide (GO).

**Acknowledgments** This research was supported by World Class University (WCU) and US-Korea NBIT programs through the National Research Foundation (NRF) of Korea funded by the Ministry of Education, Science and Technology (MEST) and US Air Force Office of Scientific Research (AFOSR).

**Open Access** This article is distributed under the terms of the Creative Commons Attribution Noncommercial License which permits any noncommercial use, distribution, and reproduction in any medium, provided the original author(s) and source are credited.

## References

1. A.K. Geim, K.S. Novoselov, Nat. Mater. **6**, 183 (2007)
2. M.S. Dresselhaus, G. Dresselhaus, Adv. Phys. **51**, 1 (2002)
3. K.S. Novoselov, A.K. Geim, S.V. Morozov, D. Jiang, Y. Zhang, S.V. Dubonos, I.V. Grigorieva, A.A. Firsov, Science **306**, 666 (2004)

4. K.S. Novoselov, A.K. Geim, S.V. Morozov, D. Jiang, M.I. Katsnelson, I.V. Grigorieva, S.V. Dubonos, A.A. Firsov, *Nature* **438**, 197 (2005)
5. Y.B. Zhang, Y.W. Tan, H.L. Stormer, P. Kim, *Nature* **438**, 201 (2005)
6. Y. Zhang, J.P. Small, M.E.S. Amori, P. Kim, *Phys. Rev. Lett.* **94**, 176803 (2005)
7. R.R. Nair, P. Blake, A.N. Grigorenko, K.S. Novoselov, T.J. Booth, T. Stauber, N.M.R. Peres, A.K. Geim, *Science* **320**, 1308 (2008)
8. S. Stankovich, D.A. Dikin, G.H.B. Dommett, K.A. Kohlhaas, E.J. Zimney, E.A. Stach, R.D. Piner, S.T. Nguyen, R.S. Ruoff, *Nature* **442**, 282 (2006)
9. S. Stankovich, R.D. Piner, S.T. Nguyen, R.S. Ruoff, *Carbon* **44**, 3342 (2006)
10. D.W. Boukhvalov, M.I. Katsnelson, *J. Am. Chem. Soc.* **130**, 10697 (2008)
11. Ç.Ö. Girit, J. Meyer, R. Erni, M.D. Rossell, C. Kisielowski, L. Yang, C.-H. Park, M.F. Crommie, M.L. Cohen, S.G. Louie, A. Zettl, *Science* **323**, 1705 (2009)
12. J.-B. Baek, C.B. Lyons, L.-S. Tan, *J. Mater. Chem.* **14**, 2052 (2004)
13. J.-B. Baek, C.B. Lyons, L.-S. Tan, *Macromolecules* **37**, 8278 (2004)
14. H.-J. Lee, S.-J. Oh, J.-Y. Choi, J.W. Kim, J. Han, L.-S. Tan, J.-B. Baek, *Chem. Mater.* **17**, 5057 (2005)
15. S.-J. Oh, H.-J. Lee, D.-K. Keum, S.-W. Lee, D.H. Wang, S.-Y. Park, L.-S. Tan, J.-B. Baek, *Polymer* **47**, 1131 (2006)
16. J.-Y. Choi, S.-J. Oh, H.-J. Lee, D.H. Wang, L.-S. Tan, J.-B. Baek, *Macromolecules* **40**, 4474 (2007)
17. H.-J. Lee, S.-W. Han, Y.-D. Kwon, L.-S. Tan, J.-B. Baek, *Carbon* **46**, 1850 (2008)
18. S.-W. Han, S.-J. Oh, L.-S. Tan, J.-B. Baek, *Carbon* **46**, 1841 (2008)
19. S.-W. Han, S.-J. Oh, L.-S. Tan, J.-B. Baek, *Nanoscale Res. Lett.* **4**, 766 (2009)
20. K. Saeed, S.-Y. Park, S. Haider, J.-B. Baek, *Nanoscale Res. Lett.* **4**, 39 (2009)
21. D.-H. Lim, C.B. Lyons, L.-S. Tan, J.-B. Baek, *J. Phys. Chem. C* **122**, 12188 (2008)
22. Q. Chen, L. Dai, M. Gao, S. Huang, A.W.H. Mau, *J. Phys. Chem. B* **105**, 618 (2001)